NOAA Technical Report NOS 83 NGS 14

Tidal Corrections to Geodetic Quantities

Rockville, Md.
February 1980

U.S. DEPARTMENT OF COMMERCE
National Oceanic and Atmospheric Administration
National Ocean Survey

NOAA Technical Publications

National Ocean Survey/National Geodetic Survey subseries

The National Geodetic Survey (NGS) of the National Ocean Survey (NOS), NOAA, establishes and maintains the basic National horizontal and vertical networks of geodetic control and provides governmentwide leadership in the improvement of geodetic surveying methods and instrumentation, coordinates operations to assure network development, and provides specifications and criteria for survey operations by Federal, State, and other agencies.

NGS engages in research and development for the improvement of knowledge of the figure of the Earth and its gravity field, and has the responsibility to procure geodetic data from all sources, process these data, and make them generally available to users through a central data base.

NOAA Technical Memorandums and some special NOAA publications are sold by the National Technical Information Service (NTIS) in paper copy and microfiche. Orders should be directed to NTIS, 5285 Port Royal Road, Springfield, VA 22161 (telephone: 703-557-4650). NTIS customer charge accounts are invited; some commercial charge accounts are accepted. When ordering, give the NTIS accession number (which begins with PB) shown in parentheses in the following citations.

Paper copies of NOAA Technical Reports that are of general interest to the public, are sold by the Superintendent of Documents, U.S. Government Printing Office (GPO), Washington, DC 20402 (telephone: 202-783-3238). For prompt service, please furnish the GPO stock number with your order. If a citation does not carry this number, then the publication is not sold by GPO. All NOAA Technical Reports may be purchased from NTIS in hard copy and microform. Prices for the same publication may vary between the two Government sales agents. Although both are nonprofit, GPO relies on some Federal support whereas NTIS is self-sustained.

An excellent reference source for Government publications is the National Depository Library program, a network of about 1,300 designated libraries. Requests for borrowing Depository Library material may be made through your local library. A free listing of libraries currently in this system is available from the Library Division, U.S. Government Printing Office, 5236 Eisenhower Ave., Alexandria, VA 22304 (telephone: 703-557-9013).

NOAA geodetic publications

Classification, Standards of Accuracy, and General Specifications of Geodetic Control Surveys. Federal Geodetic Control Committee, John O. Phillips (Chairman), Department of Commerce, NOAA, NOS, 1974 reprinted annually, 12 pp (PB265442). National specifications and tables show the closures required and tolerances permitted for first-, second-, and third-order geodetic control surveys. (A single free copy can be obtained, upon request, from the National Geodetic Survey, C18x2, NOS/NOAA, Rockville MD 20852.)

Specifications To Support Classification, Standards of Accuracy, and General Specifications of Geodetic Control Surveys. Federal Geodetic Control Committee, John O. Phillips (Chairman), Department of Commerce, NOAA, NOS, 1975, reprinted annually, 30 pp (PB261037). This publication provides the rationale behind the original publication, "Classification, Standards of Accuracy, ..." cited above. (A single free copy can be otained, upon request, from the National Geodetic Survey, C18x2, NOS/NOAA, Rockville MD 20852.)

Proceedings of the Second International Symposium on Problems Related to the Redefinition of North American Geodetic Networks. Sponsored by U.S. Department of Commerce; Department of Energy, Mines and Resources (Canada); and Danish Geodetic Institute; Arlington, Va., 1978, 658 pp. (GPO #003-017-0426-1). Fifty-four papers present the progress of the new adjustment of the North American Datum at midpoint, including reports by participating nations, software descriptions, and theoretical considerations.

NOAA Technical Memorandums, NOS/NGS subseries

NOS NGS-1 Use of climatological and meteorological data in the planning and execution of National Geodetic Survey field operations. Robert J. Leffler, December 1975, 30 pp (PB249677). Availability, pertinence, uses, and procedures for using climatological and meteorological data are discussed as applicable to NGS field operations.

NOS NGS-2 Final report on responses to geodetic data questionnaire. John F. Spencer, Jr., March 1976, 39 pp (PB254641). Responses (20%) to a geodetic data questionnaire, mailed to 36,000 U.S. land surveyors, are analyzed for projecting future geodetic data needs.

(Continued at end of publication)

NOAA Technical Report NOS 83 NGS 14

Tidal Corrections to Geodetic Quantities

P. Vaníček

National Geodetic Survey
Rockville, Md.
February 1980

U.S. DEPARTMENT OF COMMERCE
Philip M. Klutznick, Secretary

National Oceanic and Atmospheric Administration
Richard A. Frank, Administrator

National Ocean Survey
Herbert R. Lippold, Jr., Director

CONTENTS

Figures

TIDAL CORRECTIONS TO GEODETIC QUANTITIES

P. Vaníček[1]
National Geodetic Survey
National Ocean Survey, NOAA
Rockville, Md. 20852

ABSTRACT. The origin of tidal force is explained and mathematically treated. Then the phenomena caused by tidal force are shown, first by viewing the Earth as rigid and then elastic. This study is mainly devoted to the formulation of corrections arising from these tidal phenomena, and includes the complete range of geodetic observations and corrections. Finally, corrections for sea tide are discussed. Although no original material is presented, all tidal aspects that would be of interest to a geodesist are treated from a geodetic point of view.

TIDAL POTENTIAL

Celestial bodies exert a gravitational force on the Earth. At any point within or on the surface of the Earth, the gravitational force can be divided into two components: (1) a force equal to the gravitational force acting at the center of mass of the Earth, and (2) the remainder. This situation is depicted in figure 1.

It is easy to see that the first component of the gravitational force is responsible for the overall (orbital) motion of the Earth. The second part is a purely deforming force known as tidal force, illustrated in figure 1 by empty (⇨) arrows. Clearly, the tidal force tries to prolate the Earth in the direction of the attracting body.

Let us first concentrate on the most significant celestial body, the Moon, and denote its tidal acceleration by $\vec{g}_t^{\mathbb{C}}$. Using the law of universal attraction, the magnitude of $g_t^{\mathbb{C}}$ at A is

---

[1]This report was prepared during a 5-month period in 1978 when the author served as a Senior Scientist in Geodesy, National Research Council, National Academy of Sciences, Washington, D.C., while on leave from the University of New Brunswick, Fredericton, N.B., Canada.

$$g_t^{\mathbb{C}}(A) = \frac{GM^{\mathbb{C}}}{(\rho^{\mathbb{C}} - r_A)^2} - \frac{GM^{\mathbb{C}}}{\rho^{\mathbb{C}2}} = \frac{GM^{\mathbb{C}}}{\rho^{\mathbb{C}2}} \left[\left(1 - \frac{r_A}{\rho^{\mathbb{C}}} \right)^{-2} - 1 \right] . \qquad (1)$$

Here $M^{\mathbb{C}}$ denotes the mass of the Moon ($\sim 7.38 \times 10^{25}$ g), $\rho^{\mathbb{C}}$ is the distance to the Moon (on the average 3.84×10^{10} cm), r_A is the radius vector of A (on the average 6.37×10^{8} cm) and G is Newton's universal constant (6.67×10^{-8} g^{-1} cm^3 s^{-2}) (Godin 1972). $g_t^{\mathbb{C}}(A) \doteq 0.111$ mgal, i.e., about 3.4 percent of the total acceleration (~ 3.3 mgal) exerted by the Moon on the Earth. The acceleration is, of course, directed towards the Moon.

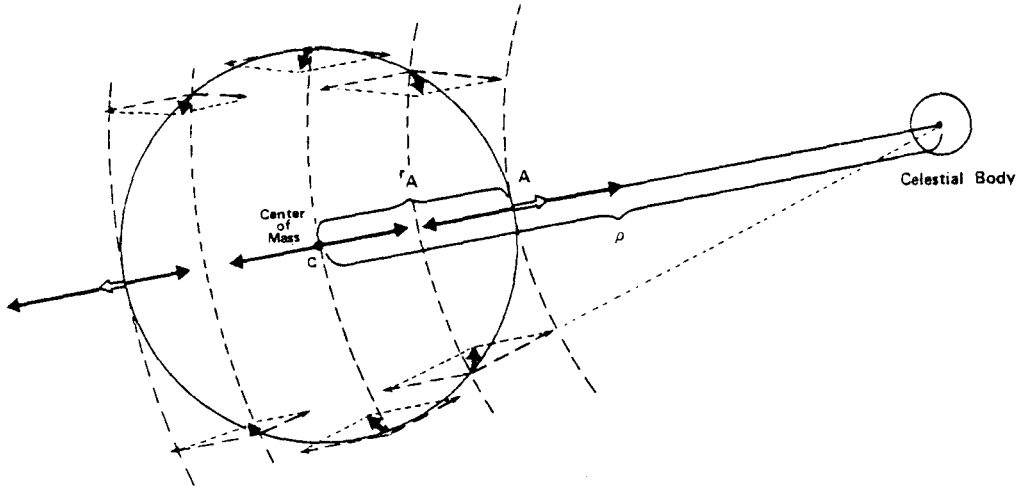

Figure 1.--Gravitational force of a celestial body exerted on the Earth. Each parallelogram is created by two vectors: one directed towards the celestial body and diminishing with distance from it, and one equal in length to the celestial body but directed in an opposite direction.

Tidal potential can be similarly evaluated as the difference between the potential of the total force and the potential of the force exerted at the center of mass. The potential of the total Moon-generated force (at A) is simply

$$W^{\mathbb{C}}(A) = \frac{GM^{\mathbb{C}}}{\rho_A^{\mathbb{C}}} = \frac{GM^{\mathbb{C}}}{(\rho^{\mathbb{C}2} + r_A^2 - 2\rho^{\mathbb{C}} r_A \cos \kappa_A^{\mathbb{C}})^{\frac{1}{2}}} \qquad (2)$$

which is graphically shown in figure 2.

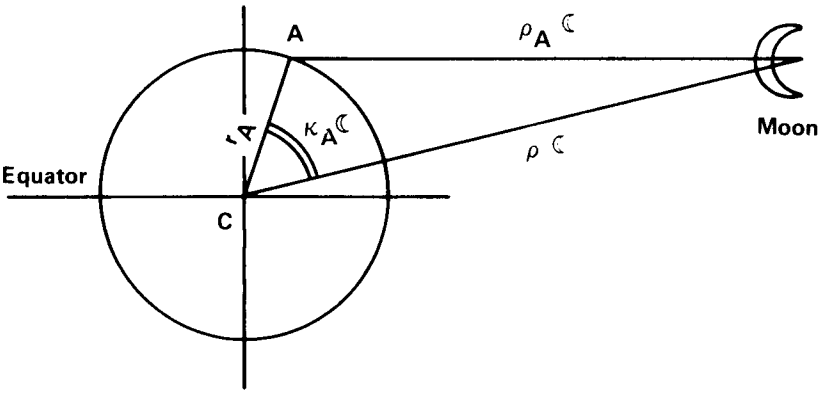

Figure 2.--Tidal potential.

Using Legendre polynomials, eq. (2) becomes

$$W^{\mathbb{C}}(A) = \frac{GM^{\mathbb{C}}}{\rho^{\mathbb{C}}} \sum_{n=0}^{\infty} \left(\frac{r_A}{\rho^{\mathbb{C}}}\right)^n P_n (\cos \kappa_A)^{\mathbb{C}}. \qquad (3)$$

The second potential is the potential of the constant field, $\vec{g}_t^{\mathbb{C}}(C)$:

$$V^{\mathbb{C}}(A) = \frac{GM^{\mathbb{C}}}{\rho^{\mathbb{C}}} + \frac{GM^{\mathbb{C}}}{\rho^{\mathbb{C}2}} r_A \cos \kappa_A = \frac{GM^{\mathbb{C}}}{\rho^{\mathbb{C}}} \sum_{n=0}^{1} \left(\frac{r_A}{\rho^{\mathbb{C}}}\right)^n P_n (\cos \kappa_A^{\mathbb{C}}). \qquad (4)$$

Thus, the lunar tidal potential is

$$W_t^{\mathbb{C}}(A) = W^{\mathbb{C}}(A) - V^{\mathbb{C}}(A) = \frac{GM^{\mathbb{C}}}{\rho^{\mathbb{C}}} \sum_{n=2}^{\infty} \left(\frac{r_A}{\rho}\right)^n P_n (\cos \kappa_A^{\mathbb{C}}). \qquad (5)$$

An identical expression can be written for solar tidal potential $W_t^{\odot}(A)$, using $M^{\odot}$, $\rho^{\odot}$, $\kappa_A^{\odot}$.

The summation W_t of lunar and solar tidal potentials, called the luni-solar potential, accounts for almost all of the tide. The largest contribution from other celestial bodies comes from the planet Venus, which amounts to about $5 \times 10^{-5} W_t$. Thus, we can ignore all remaining celestial bodies.

For geodetic applications it is sufficient to know the accuracy of the tidal potential to a few percent. At this accuracy it suffices to take only the first term in the potential development, eq. (5), because the (n+1)-st term is r/ρ times smaller than the n-th term. The third lunar term is already smaller than 0.02 times the second term. Convergence for the Sun is much faster. Hence we will use the following approximation throughout this report:

$$W_t \doteq W_2 = W_2^{\mathbb{C}} + W_2^{\odot}. \tag{6}$$

Let us now look at the temporal and geographical behavior of the tidal potential. For this purpose it is convenient to introduce the following constant (Doodson 1922):

$$D = \frac{3}{4} GM^{\mathbb{C}} \frac{R^2}{(C^{\mathbb{C}})^3} \tag{7}$$

where R is the mean (equivoluminous) radius of the Earth and $C^{\mathbb{C}}$ is the mean distance of the Moon. The value of Doodson tidal constant is

$$D \doteq 2.6277 \times 10^7 \text{ cm mgal} \tag{8}$$

which is based on the astronomic constants adopted in 1967 (Melchior 1978). Using the Doodson constant, $W_2^{\mathbb{C}}$ can be rewritten as

$$W_2^{\mathbb{C}} \doteq 2D \left(\frac{r}{R}\right)^2 \left(\frac{C^{\mathbb{C}}}{\rho}\right)^3 \left(\cos^2 \kappa^{\mathbb{C}} - \frac{1}{3}\right). \tag{9}$$

Because the two ratios depart only slightly from 1, we can write with sufficient accuracy

$$W_2^{\mathbb{C}} \doteq 2D^{\mathbb{C}} \left(\cos^2 \kappa^{\mathbb{C}} - \frac{1}{3}\right). \tag{10}$$

A similar equation holds for the Sun, where the Doodson (solar) constant equals about 46 percent of the Doodson lunar constant.

The trigonometric term can now be expressed as a function of geographic position and the position of the Moon or Sun. Using the cosine law of the nautical triangle (Mueller 1969), we get

$$\cos \kappa^{\mathbb{C}} = \sin \phi \sin \delta^{\mathbb{C}} + \cos \phi \cos \delta^{\mathbb{C}} \cos t^{\mathbb{C}} \tag{11}$$

where ϕ is the latitude of the observer, $\delta^{\mathbb{C}}$ is the declination of the Moon, and $t^{\mathbb{C}}$ its hour angle. After some simple, but lengthy, algebraic operations, we arrive at the following formula (Vaníček 1973)

$$\begin{aligned} W_2^{\mathbb{C}} \doteq D \Big[& \cos^2 \phi \cos^2 \delta^{\mathbb{C}} \cos 2t^{\mathbb{C}} + \sin 2\phi \sin 2\delta^{\mathbb{C}} \cos t^{\mathbb{C}} \\ & + 3(\sin^2 \phi - 1/3)(\sin^2 \delta^{\mathbb{C}} - 1/3) \Big] \\ = D & (S^{\mathbb{C}} + T^{\mathbb{C}} + Z^{\mathbb{C}}). \end{aligned} \tag{12}$$

The fastest time variations come from $t^{\mathbb{C}}$. The three constituents are known as sectorial (with semidiurnal frequencies), tesseral (with diurnal frequencies), and zonal (with low frequencies). An identical development can be carried out for the solar contribution.

The temporal behavior of the tidal potential, W_2, can then be best visualized in the frequency domain. Both $W_2^{\mathbb{C}}$ and $W_2^{\odot}$ time variations are concentrated in three frequency bands governed by the appropriate functions of t: low, diurnal, and semidiurnal. Within each band, some particularly notable frequencies, or periods, are distinguishable. Figure 3 depicts the spectrum containing the five major semidiurnal and diurnal frequencies

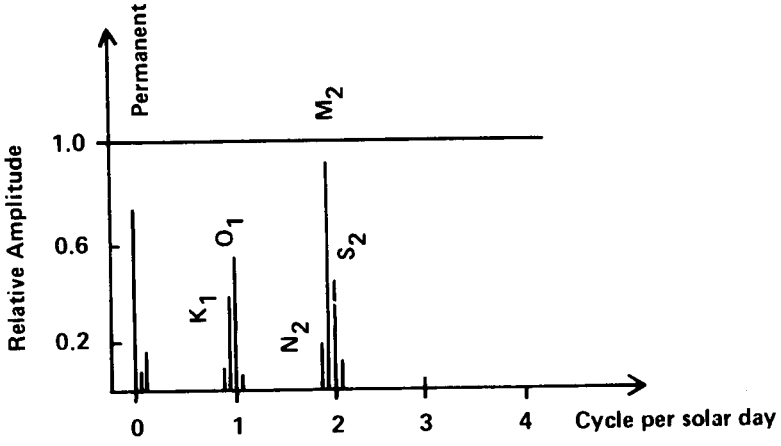

Figure 3.--Frequency spectrum of major semidiurnal and diurnal frequencies.

(M_2,S_2,N_2,O_1,K_1) plus some minor ones, according to Godin (1972). The lunar semidiurnal component (M_2) is by far the most dominant. The effect of the geographical position of the observer, i.e., the geographical effect, is explicitly expressed through latitude only. (See eq. (12).) The longitudinal dependence is hidden in the phase lag of the hour angle, t. Thus the tidal magnitude does not depend on longitude; same latitudes experience tidal effects of the same magnitude. Latitude dependence differs for sectorial and tesseral constituents. Figure 4 shows the latitude of dependence for the five major waves.

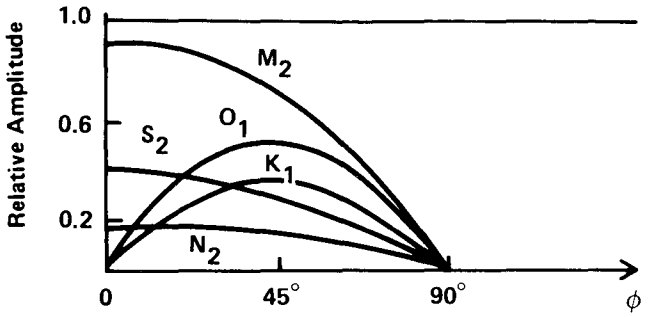

Figure 4.--Latitude variations of tidal waves.

TIDAL PHENOMENA ON THE RIGID EARTH

Tidal potential induces various observable tidal phenomena that are responsible, in turn, for the effects on various geodetic quantities. These tidal phenomena may be somewhat arbitrarily identified as being of three basic kinds: tidal gravity variations, tidal tilt, and tidal uplift. These phenomena are used here simply for mathematical convenience.

The tidal variation in gravity is the simplest phenomenon. Its magnitude was already evaluated in eq. (1). The radial component of the tidal acceleration is practically normal to the equipotential surface of the Earth's gravity field and, as such, can be computed from the following formula (e.g., for the Moon)

$$g_t^{\mathfrak{C}} \doteq -\frac{\partial W_t^{\mathfrak{C}}}{\partial r} = -\frac{GM^{\mathfrak{C}}}{r\rho^{\mathfrak{C}}} \sum_{n=2}^{\infty} n\left(\frac{r}{\rho^{\mathfrak{C}}}\right)^n P_n(\cos \kappa^{\mathfrak{C}}). \qquad (13)$$

On the Earth's surface ($r \doteq R$), we have approximately

$$g_t^{\ell} \doteq -\frac{2GM^{\ell}R}{\rho^{\ell 3}} P_2 (\cos \kappa^{\ell})$$
$$\doteq -\frac{8D}{3R} (\cos^2 \kappa^{\ell} - 1/3) \doteq -110.0 \ \mu\text{gal} \ (\cos^2 \kappa^{\ell} - 1/3). \quad (14)$$

This approach does not account for the Earth yielding under tidal stress; i.e., it considers the Earth rigid. We shall see how to correct for this later.

The derivation of tidal tilt on an equipotential surface is slightly more involved. Figure 5 shows the tilt is equal to

$$\theta_t \doteq \frac{(g_t)_{hor}}{g} . \quad (15)$$

The horizontal component of tidal gravity (fig. 2) is simply

$$(g_t)_{hor} = \frac{\partial W_t}{r \, \partial \kappa}. \quad (16)$$

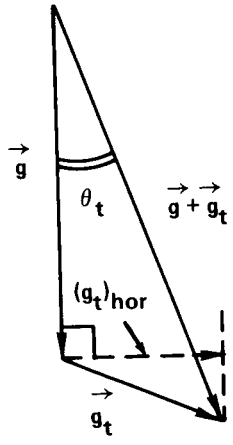

Figure 5.--Tidal tilt of an equipotential surface.

Maximum tilt occurs in the plane that contains the Earth's center of mass, the observer, and the attracting body. Tilt in the α direction is then calculated from a formula parallel to that used for the projection of the deflection of the vertical θ to the α direction (Bomford 1971).

Using the usual geodetic sign convention,

$$\theta_t(\alpha) = -\frac{1}{gR}\left(\cos\alpha\,\frac{\partial W_t}{\partial\phi} + \sin\alpha\,\frac{\partial W_t}{\cos\phi\,\partial\lambda}\right). \tag{17}$$

On the Earth's surface, the lunar contribution for the rigid Earth is

$$\begin{aligned}\theta_t^{\mathbb{C}}(\alpha) &\doteq -\frac{2D}{gR}\left(\cos\alpha\,\frac{\partial\cos^2\kappa^{\mathbb{C}}}{\partial\phi} + \sin\alpha\,\frac{\partial\cos^2\kappa^{\mathbb{C}}}{\cos\phi\,\partial\lambda}\right)\\ &\doteq -0''.017\left(\cos\alpha\,\frac{\partial\cos^2\kappa^{\mathbb{C}}}{\partial\phi} + \sin\alpha\,\frac{\partial\cos^2\kappa^{\mathbb{C}}}{\cos\phi\,\partial\lambda}\right).\end{aligned} \tag{18}$$

Finally, the tidal uplift of an equipotential surface (fig. 6) is given by using the well-known formula of potential theory:

$$u_t = \frac{W_t}{g}. \tag{19}$$

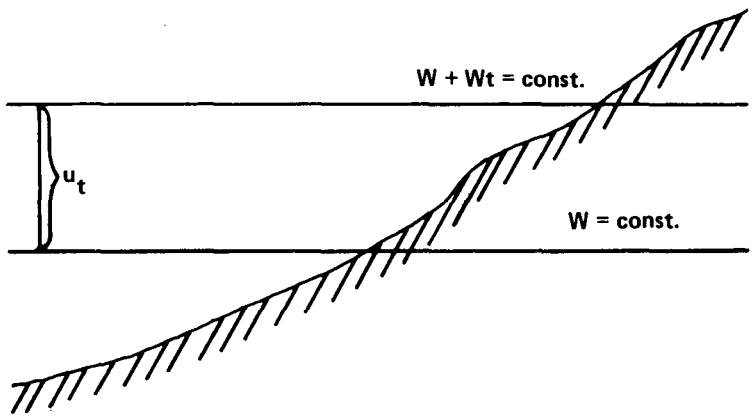

Figure 6.--Tidal uplift of an equipotential surface.

This is an application of the general formula, $g = \frac{\partial W}{\partial n}$. (See for example, Heiskanen and Moritz (1967).) Thus, for instance,

$$u_t^{\mathbb{C}} = \frac{GM^{\mathbb{C}}}{g\rho^{\mathbb{C}}}\sum_{n=2}^{\infty}\left(\frac{r}{\rho^{\mathbb{C}}}\right)^n P_n(\cos\kappa^{\mathbb{C}}). \tag{20}$$

On the Earth's surface (again for the rigid Earth only), we get

$$u_t^{\mathbb{C}} \doteq \frac{2D}{g} (\cos^2 \kappa^{\mathbb{C}} + 1/3)$$

$$\doteq 53.6 \text{ cm } (\cos^2 \kappa^{\mathbb{C}} + 1/3). \qquad (21)$$

For the rigid Earth the tidal uplift also describes the amount of water tide. Theoretically, ignoring the inhomogeneity of water, in response to tidal stress water constantly adjusts its level to coincide with an equipotential surface. This is seldom the case in nature because water becomes trapped by the shores, which restricts its movement. Thus water tends to pile up in constricted areas. This effect is more pronounced in shallow seas where the magnitude of the sea tide is particularly affected by local conditions and often magnified out of proportion.

Although the amplitudes become completely distorted, the frequencies do not. Frequencies of the sea tide reproduce quite closely the frequencies of the tidal potential. Amplitudes and phases of the sea tide must be determined from observations. Characteristics of the sea tide are observed on shore with tide gages. Then tides on the open seas are mathematically modeled, thereby giving cotidal charts or models for different tidal frequencies.

Sea tides, i.e., the tidal waters of the seas, have their own effect on geodetic quantities even on solid land. To distinguish between these two sets of effects, we will talk about tidal effects (perturbations) and sea tide effects (perturbations). The first set of effects is sometimes referred to in the literature as "body tide" effects, the second as "tidal loading" effects.

TIDAL PHENOMENA ON THE DEFORMABLE EARTH

So far, we have assumed that the Earth is rigid; we have not allowed it to respond to stress or to any secondary effect of an induced deformation. The

following question then arises: What will be the magnitude of the various tidal phenomena on the surface of the real, yielding Earth? For deformations of a relatively short periodic nature, such as tides, it is believed that the Earth responds essentially in an elastic manner. The visco-elastic model is usually stipulated only for stresses of a longer period.

To show how the elasticity of the Earth affects tidal phenomena, let us first discuss tidal uplift. The ratio of the radial elastic displacement of a mass element of the Earth to the radial displacement of the corresponding element of a hypothetical fluid Earth is called the first Love number, denoted by h. Therefore, a fluid Earth would be characterized by h = 1. An absolutely rigid Earth would have h = 0. The actual Earth displays Love numbers between 0 and 1, depending on the spatial wavelength of the deforming force and on depth. Only the surface value h_2 for wave number 2 is of interest to the geodesist because only the Earth's surface and the second harmonic tidal potential W_2 are used. h_2 equals about 0.62 (Melchior 1978). This value was determined from observations of tidal response on diurnal and semidiurnal frequencies, and is denoted simply by h.

The ratio of the tangential elastic displacement of an actual mass element to the corresponding displacement of its hypothetical fluid counterpart is known as Shida's number, denoted by ℓ. For this purpose the Earth is considered to be isotropic within each layer, i.e., responding in the same manner in all directions. The isotropic Shida's number, like the first Love number, varies only with the wavelength of the deforming force and depth. On the Earth's surface the value of ℓ_2 is about 0.08 (Ozawa 1965), determined again from analysis of tidal deformations. We will again use only ℓ_2 and call it ℓ.

The shape of the real Earth changes in response to tidal stress, which means that a redistribution of the Earth's masses occurs. Naturally, this redistribution must also change the Earth's own gravity field. This change, expressed as a change in the Earth's potential, is called the deformation potential W_d. Its effect is most clearly seen on tidal uplift: It magnifies

the calculated value u_t by a factor $1 + k > 1$. Referring to eq. (19), the uplift affected by the deformation potential is written as

$$u_t(1+k) = \frac{W_t + W_d}{g}. \tag{22}$$

Thus

$$k = W_d/W_t. \tag{23}$$

This ratio is called the second Love number. Its effect is shown in figure 7. The determined value for wave number 2 is about 0.29 (Melchior 1978) from tidal observations of gravity and tilt.

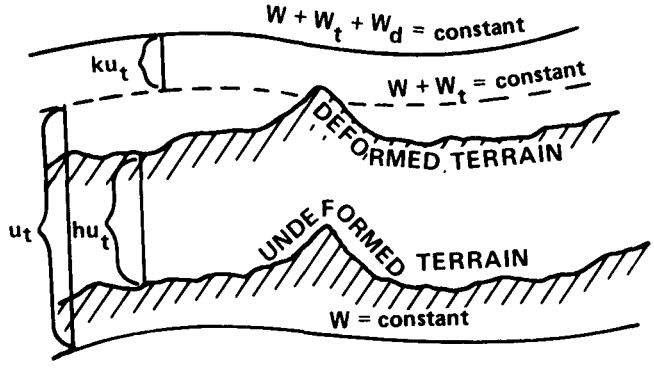

Figure 7.--Tidal uplift for deformed terrain.

Evidently, by responding to deformation potential the Earth changes its shape, and thus the effect of tidal stress changes as well. This, in turn, causes an additional deformation potential. What we observe is, of course, the final deformation after the equilibrium has been reached. The values of all the Love numbers, including Shida's number (normally referred to as one of the Love numbers), then reflect the equilibrium state.

It is easily seen that all tidal phenomena are affected by the deformability of the Earth. In addition, many more tidal effects are distinguishable on the deformable Earth than on the rigid Earth. For example, for the rigid

Earth we could only consider the tilt of an equipotential surface; now we can also determine the tilt of the Earth's surface as well as the relative tilt of these two. Rather than dwelling on this point, let us treat these effects in the context of geodetic quantities.

TIDAL CORRECTIONS TO GEODETIC QUANTITIES

The following geodetic quantities are subject to tidal corrections:

- geocentric height
- geoidal height
- orthometric or normal height
- sea level
- absolute gravity
- relative gravity
- distances
- horizontal angles
- astronomic deflections of the vertical
- tilt of the Earth's surface
- relative tilt of the Earth's surface
- leveled height differences
- vertical angles

• Geocentric height, r, of a terrain point (fig. 7) is evidently affected by

$$\delta r_t = h u_t . \tag{24}$$

The correction to instantaneous geocentric height (correction defined as effect taken with negative sign) is

$$O r_t \doteq - \frac{0.62}{g} W_2 \doteq - 0.63 \times 10^{-6} \text{ mgal}^{-1} W_2 . \tag{25}$$

• Geoidal height, N, above a fixed geocentric ellipsoid is given by eq. (22). The correction to the instantaneous geoid can be written as

$$O N_t \doteq - (1+k) W_2/g = - \frac{1.29}{g} W_2 \doteq -1.32 \times 10^{-6} \text{ mgal}^{-1} W_2 . \tag{26}$$

By applying this correction, we arrive at a mean geoidal height (in time).

• Orthometric or normal height, H, is clearly affected by both of the two previous effects. Subtracting these effects we get

$$OH_t = [h-(1+k)]\ u_t. \tag{27}$$

The correction to instantaneous orthometric (normal) height is then

$$OH_t \doteq \frac{0.67}{g} W_2 \doteq 0.68 \times 10^{-6}\ \text{mgal}^{-1}\ W_2. \tag{28}$$

• Sea-level height, Z, observed from the shore is affected by the same amount as orthometric height but with an opposite sign. However, this correction is never used because the tidal amplitudes are much more disturbed by dynamic phenomena and, in any case, the distortions cannot be separated. Therefore, if needed, the actually observed amplitudes are used.

• Absolute gravity changes, g_t^*, i.e., changes of gravity at a point fixed with respect to a geocentric coordinate system, are given by the familiar equation:

$$g_t^* \doteq - \frac{\partial}{\partial r} (W_t + W_d). \tag{29}$$

Limiting ourselves to only W_2, we can write

$$g_t^* \doteq - \frac{\partial}{\partial r} (W_2 + kW_2) = - (1+k) \frac{\partial W_2}{\partial r} - W_2 \frac{\partial k}{\partial r}. \tag{30}$$

It has been shown that for W_2 within the Earth, k must be proportionate to r^{-5} (Love 1927) so that

$$\frac{\partial k}{\partial r} = - \frac{5k}{r}. \tag{31}$$

Realizing that

$$\frac{W_2}{r} = 1/2 \ \frac{\partial W_2}{\partial r} \tag{32}$$

we get finally

$$g_t^* \doteq - (1 - 3/2k) \frac{\partial W_2}{\partial r}. \tag{33}$$

On the Earth's surface ($r \doteq R$), we get the correction

$$0g_t^* \doteq \frac{0.565}{R} 2W_2 \doteq 0.18 \times 10^{-8} \text{ cm}^{-1} W_2. \tag{34}$$

• Relative gravity changes, $\tilde{g}_t$, i.e., changes observed with an instrument attached to the Earth's surface, also reflect the vertical movement of the Earth's surface. We then must account for the movement of the instrument through the gravity field, δr_t. The additional gravity change resulting from this vertical shift is equal to

$$\delta r_t \frac{\partial g}{\partial r} \doteq - h \frac{W_2}{g} \frac{2g}{R} = - h \frac{2W_2}{R}. \tag{35}$$

Combining this with eq. (33),

$$\tilde{g}_t \doteq (1 + h - 3/2k) \frac{2W_2}{R} \tag{36}$$

and the appropriate correction is

$$0\tilde{g}_t \doteq \frac{1.185}{R} 2W_2 \doteq 0.37 \times 10^{-8} \text{ cm}^{-1} W_2. \tag{37}$$

• Distances, d, on the Earth's surface are affected in a different manner for different azimuths and tidal frequencies. To derive these expressions we must first derive the tidal strain tensor. If the displacement vector of a mass element within the Earth is denoted by $\vec{v}$, then for the following matrix (Condon and Odishaw 1958)

$$\underline{\varepsilon} = \tfrac{1}{2} (\nabla \vec{v}^T) (\nabla \vec{v}^T)^T \tag{38}$$

where ∇ is the first-order differential operator, and can be regarded as the strain tensor corresponding to the displacement $\vec{v}$. For geodetic coordinates, it is stated as

$$\underline{\varepsilon} = \begin{bmatrix} e_{rr}, & e_{r\phi}, & e_{r\lambda} \\ e_{\phi r}, & e_{\phi\phi}, & e_{\phi\lambda} \\ e_{\lambda r}, & e_{\lambda\phi}, & e_{\lambda\lambda} \end{bmatrix} \tag{39}$$

where, according to Love (1927) (and replacing the second spherical coordinate by $\pi/2 - \phi$):

$$e_{rr} = \frac{\partial v_r}{\partial r}$$

$$e_{r\phi} = e_{\phi r} \doteq \frac{\partial v_\phi}{\partial r} - \frac{v_\phi}{r} + \frac{\partial v_r}{r\partial\phi}$$

$$e_{r\lambda} = e_{\lambda r} \doteq \frac{1}{r\cos\phi}\frac{\partial v_r}{\partial\lambda} + \frac{\partial v_\lambda}{\partial r} - \frac{v_\lambda}{r}$$

$$e_{\phi\phi} \doteq \frac{\partial v_\phi}{r\partial\phi} + \frac{v_r}{r}$$

$$e_{\phi\lambda} = e_{\lambda\phi} \doteq \frac{\partial v_\lambda}{r\partial\phi} - \tan\phi\,\frac{v_\lambda}{r} + \frac{1}{r\cos\phi}\frac{\partial v_\phi}{\partial\lambda}$$

$$e_{\lambda\lambda} \doteq \frac{1}{r\cos\phi}\frac{\partial v_\lambda}{\partial\lambda} + \tan\phi\,\frac{v_\phi}{r} + \frac{v_r}{r}.$$

On the Earth's surface it is logical to speak of surface strain as being characterized by the following two-dimensional tensor

$$\underline{\varepsilon}' = \begin{bmatrix} e_{\phi\phi}, & e_{\phi\lambda} \\ e_{\lambda\phi}, & e_{\lambda\lambda} \end{bmatrix}. \tag{40}$$

Let us now consider the displacement vector in terms of tidal potential, i.e.,

$$v_r = \delta r_t = h u_t = h \frac{W_t}{g}$$

$$v_\phi = \frac{\ell}{g} \frac{\partial W_t}{\partial \phi} \tag{41}$$

$$v_\lambda = \frac{\ell}{g} \frac{\partial W_t}{\cos \phi \partial \lambda} .$$

For eqs. (40) and (41) refer to Melchior (1978). After some rearranging we obtain

$$\underline{\varepsilon}' \doteq \frac{h}{Rg} \underline{I} W_t + \frac{\ell}{Rg} \underline{D}^2 (W_t). \tag{42}$$

Here $\underline{D}^2$ is the following matrix differential operator

$$\underline{D}^2 = \begin{bmatrix} \dfrac{\partial^2}{\partial \phi^2} & , & -\dfrac{2}{\cos \phi} \left(\dfrac{\partial^2}{\partial \phi \partial \lambda} + \tan \phi \dfrac{\partial}{\partial \lambda} \right) \\ -\dfrac{2}{\cos \phi} \left(\dfrac{\partial^2}{\partial \phi \partial \lambda} + \tan \phi \dfrac{\partial}{\partial \lambda} \right), & \dfrac{1}{\cos^2 \phi} & \dfrac{\partial^2}{\partial \lambda^2} + \tan \phi \dfrac{\partial}{\partial \phi} \end{bmatrix} . \tag{43}$$

Now, the relative deformation (strain) in azimuth α (Love 1927) is

$$\varepsilon_\alpha = \cos^2 \alpha \, e_{\phi\phi} + \sin^2 \alpha \, e_{\lambda\lambda} + \cos \alpha \sin \alpha \, e_{\phi\lambda}. \tag{44}$$

More concisely, denoting $(\cos\alpha, \sin\alpha)$ by $\underline{A}(\alpha)$

$$\begin{aligned} \underline{\varepsilon}^* &\doteq \frac{h}{Rg} \underline{I} W_t + \frac{\ell}{Rg} \underline{D}^{*2} (W_t) \\ &\doteq 1.0 \times 10^{-15} \text{ cm}^{-1} \text{ mgal}^{-1} \underline{I} W_2 + 1.3 \times 10^{-16} \text{ cm}^{-1} \text{ mgal}^{-1} \underline{D}^{*2} (W_2) \end{aligned} \tag{45}$$

where D^{*2} differs from $\underline{D}^2$ only by halving off-diagonal elements. We then obtain the following correction to distance d

$$0d_t = - \underline{A}^T (\alpha) \underline{\varepsilon}^* \underline{A}(\alpha) d. \tag{46}$$

The components of the strain tensor are, at most, of the order of 10^{-8}. Therefore, this correction is not necessary unless relatively very precise distances are used. At present this may be necessary only for very long base line interferometry (VLBI).

• Horizontal angles are also affected by strain. Therefore, a correction to horizontal angles may be worked out from the strain tensor, eq. (45). However, it is difficult to visualize where it might be applied.

• Astronomic deflections of the vertical, θ, are affected by the tidal effects on both the Earth's surface and the gravity field. Figure 8 depicts this situation. The effect on an equipotential surface is $(1 + k)\theta_t$. The effect on the Earth itself is only horizontal; the observation point becomes displaced by $R\ell\theta_t$. Hence, the total effect in the plane of maximum tilt is

$$\theta'_t = - (1+k-\ell)\ \theta_t = - \frac{1+k-\ell}{gR} \frac{\partial W_t}{\partial \kappa}. \tag{47}$$

Taking into account the sign convention for deflections, the corrections to astronomic deflection components are

$$\begin{aligned} 0\xi_t &= 1.94 \times 10^{-15}\ \text{cm}^{-1}\ \text{mgal}^{-1} \frac{\partial W_2}{\partial \phi} \\ 0\eta_t &= 1.94 \times 10^{-15}\ \text{cm}^{-1}\ \text{mgal}^{-1} \frac{\partial W_2}{\cos\phi \partial \lambda}. \end{aligned} \tag{48}$$

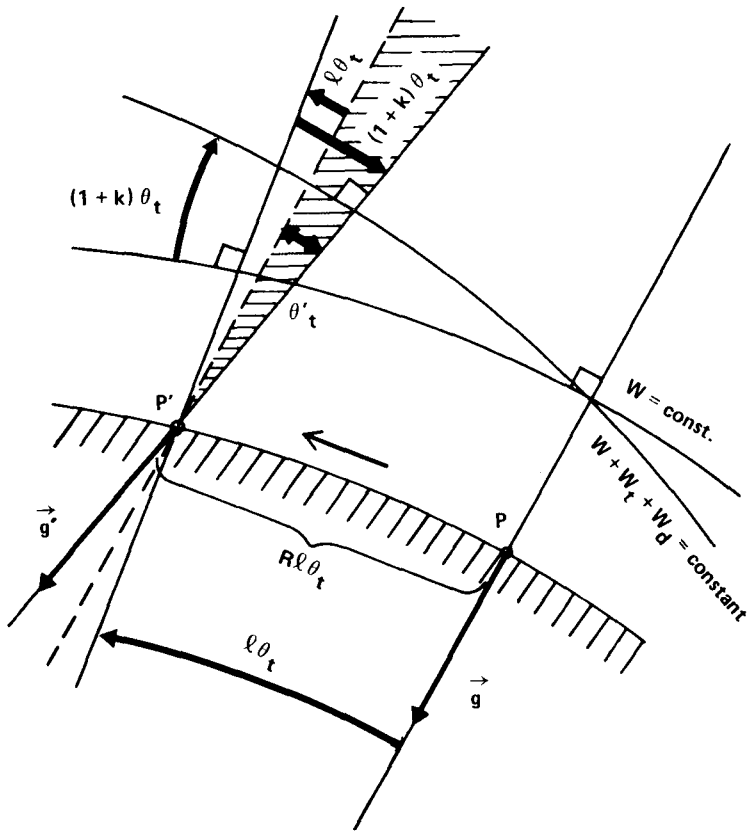

Figure 8.--Tidal effect on astronomic deflections of the vertical.

• Tilt of the Earth's surface, θ^*, measured absolutely (with respect to a geocentric coordinate system) will have the correction

$$0\theta_t^* = -h\theta_t \doteq -0.99 \times 10^{-15}\ \text{cm}^{-1}\ \text{mgal}^{-1}\ \frac{\partial W_2}{\partial \kappa}\ . \qquad (49)$$

• Relative tilt of the Earth's surface, $\tilde{\theta}$, i.e., tilt measured with respect to an equipotential surface, gives

$$0\tilde{\theta}_t = (1+k-h)\ \theta_t \doteq 1.07 \times 10^{-15}\ \text{cm}^{-1}\ \text{mgal}^{-1}\ \frac{\partial W_2}{\partial \kappa}. \qquad (50)$$

Note the reversed signs in the last two equations.

• Leveled height differences, ΔH, are affected in a manner parallel to relative tilt. Clearly, as shown in figure 9, the effect on one rod reading, F or B, is

$$\delta F_t = - \delta B_t = (1+k-h)\theta_t \frac{\Delta S}{2}. \tag{51}$$

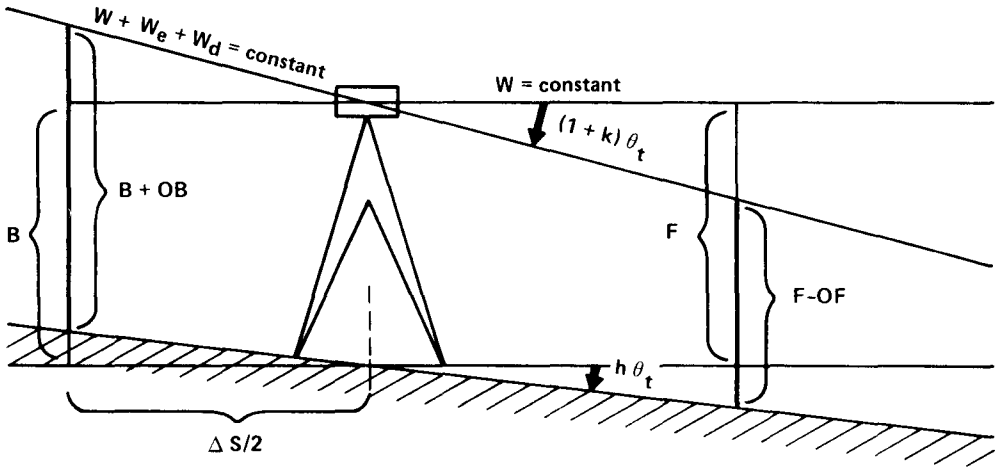

Figure 9.--Tidal effect on a leveled height difference.

Again, by accounting for the correct sign, the correction is

$$\begin{aligned} O(F-B)_t &\doteq \frac{1+k-h}{gR} \Delta S \left(\cos \alpha \frac{\partial W_2}{\partial \phi} + \sin \alpha \frac{\partial W_2}{\cos \phi \, \partial \lambda} \right) \\ &\doteq 1.07 \times 10^{-15} \text{ cm}^{-1} \text{ mgal}^{-1} \Delta S \left(\cos \alpha \frac{\partial W_2}{\partial \phi} + \sin \alpha \frac{\partial W_2}{\cos \partial \, \phi \lambda} \right). \end{aligned} \tag{52}$$

• Vertical angles, β, (and zenith distances) are affected through a change in both the astronomic deflections as well as the tilt of the Earth's surface.

All three Love numbers play their role and the correction in azimuth α is

$$0\beta_t \doteq -\frac{1+k-h-\ell}{gR}\left(\cos\alpha\,\frac{\partial W_2}{\partial\phi}+\sin\alpha\,\frac{\partial W_2}{\cos\phi\,\partial\lambda}\right)$$
$$\doteq -0.94\times10^{-15}\ \mathrm{cm^{-1}\ mgal^{-1}}\left(\cos\alpha\,\frac{\partial W_2}{\partial\phi}+\sin\alpha\,\frac{\partial W_2}{\cos\phi\partial\lambda}\right). \qquad (53)$$

Because the vertical angles are strongly affected by vertical refraction, it is difficult to see why a correction as small as the tidal correction would have to be applied.

In applying any of the previous corrections, the user must realize that none of the Love numbers is accurately known. In addition, significant local perturbations probably exist which are caused by geological inequities and topographical relief (Harrison 1978) as well as by aliasing different tidal phenomena. The corrections, however, can still be evaluated to an accuracy of about 10 percent.

Various algorithms are available for the tidal potential and its derivatives. These algorithms can readily be used to generate W_2 or even better approximations of W_t. It would be irrelevant to discuss the question here; for our purpose we assume that the software for generating tidal potential is available.

SEA-TIDE CORRECTIONS

Let us now turn to the next category of tidal effects and corrections--those caused by sea tide (tidal waters). The most conspicuous effect is water loading, i.e., the sagging of the lithosphere under the weight of additional water. The amount and extent of sagging depend on the thickness and rheological properties of the lithosphere. As an example, the sea tide observed with shore tide gages is directly affected by this phenomenon.

Two more phenomena must be considered when investigating sea tide effects: gravitational attraction of tidal waters and gravitational attraction of the

crustal deformation caused by the load. The latter is known as the indirect effect and is closely related to the deformation potential effect discussed in the preceding sections. As in the case of pure tidal phenomena, all three manifestations should be treated together because their total equilibrium state is of interest.

The easiest effect to evaluate is the gravitational attraction which requires only a knowledge of tidal water distribution, i.e., the cotidal charts, or sea tide models, and the position of the point of interest with respect to these water masses. No information on Earth rheology is necessary. This is why the attraction effect serves as a "reference effect" for the other two, a role similar to that of the fluid Earth's response in tidal theory.

The mathematical modeling of sea-tide effects is analogous to the approach used in investigating the purely tidal responses above, in that the loading effect is elastic. Also, the idea of rheological functions, similar to Love numbers, is used. Otherwise the treatment of sea-tide effects is different, mainly because the deforming forces (load and attraction) are irregularly distributed on the Earth's surface.

To explain the treatment of sea-tide effects, let us begin once more with vertical displacements. Let u_ℓ denote the vertical displacement of the Earth's surface under the load, u_a is the displacement of a gravity equipotential surface caused by the attraction of water masses, and u_i represents the indirect effect. Munk and MacDonald (1960) introduced a system of rheological functions, h', k' and ℓ', called load numbers. These are defined by the following ratios that use the attraction effect as a norm:

$$h' = u_\ell / u_a$$

$$k' = u_i / u_a \qquad (54)$$

$$\ell' = v_\ell / v_a$$

where v denotes horizontal displacement in the direction of the load.

Load numbers, like Love numbers, are functions of depth and the horizontal dimension of the load. We will deal only with surface values, but unlike previously, we will have to deal with all possible wave numbers n because of the irregularity of the sizes and shapes of the loading water masses. Load numbers corresponding to a load of infinitesimally small dimensions are denoted by h'_∞, k'_∞ and ℓ'_∞.

It is expedient to introduce the gravitational attraction potential, W_w, of the tidal waters. By denoting Z for the amplitude of the sea tide at the moment of interest, we can write the following equation for the potential at A:

$$W_w(\vec{r}_A) = - G \iint_S \frac{Z(\vec{r})\ \sigma_w}{\rho(\vec{r}_A, \vec{r})}\, dS \tag{55}$$

where $\sigma_w = 1.027\ \mathrm{gcm}^{-3}$ is the mean density of sea water. The integration is carried out over the surface, S, of the Earth, with the understanding that $Z = 0$ on land. Now the inverse chord distance ρ^{-1} can be developed into a series of Legendre polynomials, so that by using spherical approximation we get (Heiskanen and Moritz 1967)

$$W_w(\phi,\lambda) \doteq - RG\sigma_w \iint_S Z(\phi',\lambda') \sum_{n=0}^{\infty} P_n\ (\cos\ \psi)\ d\nu \tag{56}$$

where ψ is the spatial angle between (ϕ,λ) and (ϕ',λ'). The solid angle element, $d\nu$ is used for integration rather than the surface element, dS.

Because the subintegral function is well-behaved, we can interchange summation and integration, and obtain

$$W_w(\phi,\lambda) \doteq \sum_{n=0}^{\infty} - RG\sigma_w \iint_S Z(\phi',\lambda')\ P_n\ (\cos\ \psi)\ d\nu \tag{57}$$

$$= \sum_{n=0}^{\infty} (W_w)_n$$

a series of spherical harmonics. Using the identity (Rektorys 1969):

$$\sum_{n=0}^{\infty} P_n (\cos \psi) = \sqrt{2}(1 - \cos \psi)^{-\frac{1}{2}}, \tag{58}$$

then eq. (56) can be written also in the closed form:

$$W_w(\phi,\lambda) \doteq - \frac{RG\sigma_w}{\sqrt{2}} \iint_S Z(\phi',\lambda')(1- \cos \psi)^{-\frac{1}{2}} \, d\nu . \tag{59}$$

As shown in eq. (19), the vertical displacement caused by the deforming potential is

$$u_a = \frac{W_w}{g}. \tag{60}$$

Substituting for W_w, either from eqs. (57) or (59), we obtain the expression for u_a either in terms of spherical harmonics or as a convolution integral. It is illustrative to spell out the convolution integral:

$$u_a (\phi,\lambda) = \iint_S K^{ua} (\phi,\lambda,\phi',\lambda') \; Z (\phi',\lambda') \; d\nu \tag{61}$$

where the integration kernel is homogeneous and isotropic, namely

$$K^{ua} = - \frac{RG\sigma_w}{\sqrt{2}g} (1 - \cos \psi)^{-\frac{1}{2}} = - 0.0315 (1 - \cos \psi)^{-\frac{1}{2}}. \tag{62}$$

Viewed from the theory of differential equations, the integration kernel is also a Green's function and is often referred to as such in the literature.

Substituting the spherical harmonic series version of u_a in eq. (60), i.e.,

$$u_a = \frac{1}{g} \sum_{n=0}^{\infty} (W_w)_n, \tag{63}$$

into eq. (54) we obtain

$$u_\ell = \frac{1}{g} \sum_{n=0}^{\infty} h'_n (W_w)_n$$

$$u_i = \frac{1}{g} \sum_{n=0}^{\infty} k'_n (W_w)_n \tag{64}$$

and

$$v_\ell = \frac{1}{g} \sum_{n=0}^{\infty} \ell'_n \frac{\partial (W_w)_n}{\partial \psi}.$$

All of these effects now can be evaluated if the load numbers (for all the wave numbers) are known to a high enough order. There are not enough available observations of responses to loads, however, to evaluate the load numbers directly. Instead, load numbers must be evaluated from a rheological model of the Earth. The result of one such evaluation (Farrell 1972) is given in figure 10. In this illustration Farrell used the standard

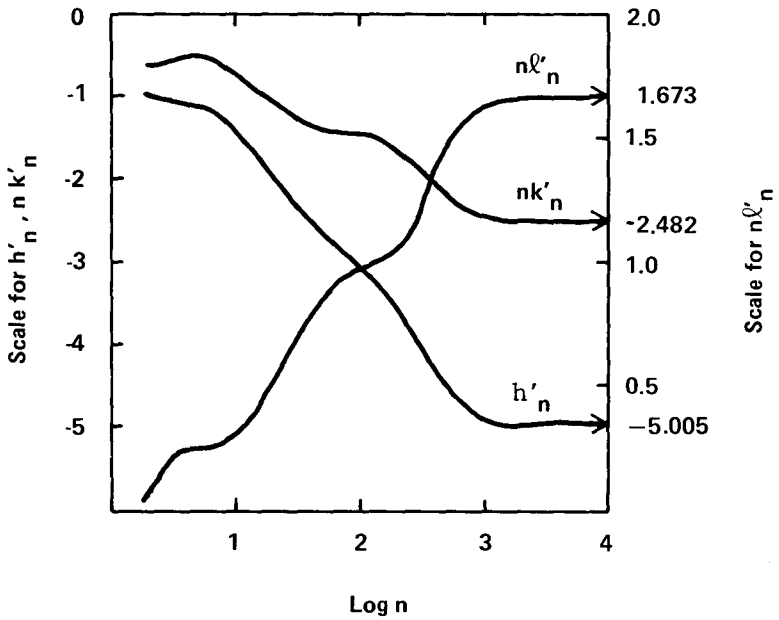

Figure 10.--Load numbers, excerpted from Farrell (1972).

Gutenberg-Bullen rheological model A of the Earth, e.g., Alterman et al. (1961).

Effects can also be evaluated from closed formulas rather than from series. Such closed formulas can be derived by the same method used to derive eq. (59). Interchanging the integration with the summation we get

$$u_\ell(\phi,\lambda) = \oiint_S K^{u\ell}(\phi,\lambda,\phi',\lambda') \; Z(\phi',\lambda') \; d\nu \tag{65}$$

where the Green's function (integration kernel) equals

$$K^{u\ell} = -\frac{RG\sigma_w}{g} \sum_{n=0}^{\infty} h'_n P_n(\cos\psi). \tag{66}$$

Again the kernel is homogeneous and isotropic.

Although the convolution integral is a better approach to the evaluation of local contributions, i.e., effect of the water masses in the close environment of the point of interest, the series approach appears more convenient for evaluating the contribution of the distant seas (for which the integration is time-consuming). Therefore, it may be useful to combine the two techniques by optimizing the ratio of accuracy to the time necessary for the evaluation. This is shown by the following reasoning.

1. Let us write the convolution integral for an effect e as:

$$e(r) = \oiint_S K^e(r,r') \; Z(r') \; d\nu'. \tag{67}$$

Leaving out the arguments, this can also be written as

$$e = \oiint_S K^e (Z-Z^N) \, d\nu' + \oiint_S K^e Z^N \, d\nu' = I_1 + I_2 \tag{68}$$

where Z^N is an approximation of Z.

2. Let

$$Z^N(r') = \sum_{n=0}^{N} c_n(Z)\, Y_n(r') = \sum_{n=0}^{N} Z_n(r') \tag{69}$$

where Y_n are the spherical harmonics and $c_n(Z)$ their coefficients.

Then the second integral can be written as

$$I_2 = \oiint_S K^e(r,r') \sum_{n=0}^{N} Z_n(r')\, d\nu'. \tag{70}$$

3. Generally the integration kernel can be expressed as

$$K^e(r,r') = \kappa^e \sum_{m=0}^{\infty} L_m^e\, P_m\, [\cos \psi(r,r')] \tag{71}$$

where K^e is the constant term appropriate for the effect e, and L_m^e is a particular linear combination of the load numbers for the effect.

4. Substitution for K^e in eq. (70) yields

$$I_2 = \oiint_S \kappa^e \sum_{m=0}^{\infty} L_m^e\, P_m\, [\cos \psi\ (r,r')] \sum_{n=0}^{N} c_n(Z)\, Y_n(r')\, d\nu'. \tag{72}$$

Then

$$I_2 = \kappa^e \sum_{n=0}^{N} \sum_{m=0}^{\infty} L_m^e\, c_n(Z) \oiint_S P_m\, [\cos \psi(r,r')]\, Y_n(r')\, d\nu'. \tag{73}$$

5. Using the Laplace decomposition formula for $P_m(\cos\psi)$, e.g., Rektorys (1969), we discover that $P_m(\cos\psi)$ is a "reproducing kernel" and

$$\iint_S P_m\left[\cos\psi(r,r')\right] Y_n(r')\, d\nu' = \delta_{nm}\, Y_n(r). \tag{74}$$

Substituting back to eq. (73), we obtain

$$I_2 = \kappa^e \sum_{n=0}^{N} L_n^e\, c_n(Z)\, Y_n(r) = \kappa^e \sum_{n=0}^{N} L_n^e\, Z_n(r). \tag{75}$$

6. If Z^N is a reasonable approximation of Z, then the convolution involved in the evaluation of I_1 does not have to be carried out over the entire Earth. It can be replaced by integration over a neighborhood E of the point of interest. Finally we obtain

$$e(r) \doteq \iint_E K^e(r,r')\left[Z(r') - \sum_{n=0}^{N} Z_n(r')\right] d\nu + \kappa^e \sum_{n=0}^{N} L_n^e\, Z_n(r). \tag{76}$$

Unfortunately, the situation is more complicated when Green's function is composed of horizontal derivatives of $P_m(\cos\psi)$, as is the case for horizontal displacement and tilt. A different approach must be used.

The widest range of Green's functions for elastic displacement (vertical and horizontal), tilt, strain, and gravity response to surface loads was computed by Farrell (1972), based on Longman's (1962, 1963) foundations. Farrell used three alternative Earth models to generate his Green's functions: the Gutenberg-Bullen model A, mentioned previously for vertically displaced Green's function (see fig. 11), and two of Harkrider's (1970) variants of the same. These differ from the Gutenberg-Bullen model by only the top 1000-km layers. Harkrider uses structures representing continental and oceanic shields, respectively. The load numbers for each of the three models are different. Nevertheless, Farrell's results indicate that except

for the nearest few hundred kilometers, the differences between the models are unimportant. They all indicate the same response to within an accuracy of a few percent.

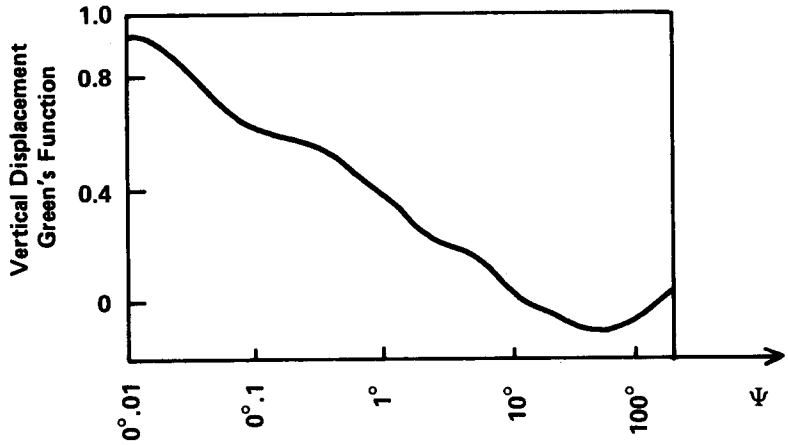

Figure 11.--Load numbers for Gutenberg-Bullen model, excerpted Farrell (1972).

Other researchers, e.g., Beaumont and Lambert (1972), and Zschau (1976), tend to support this indication. For longer distances any of the above models is adequate, but for shorter distances local geology must be taken into account. Local geology may be responsible for deviations in the response to several tens of percent from the global models. Almost no information exists at present on the probable anisotropy of the actual response. Thus, coastal areas present a definite problem in modeling the sea tide corrections. In addition to these difficulties, the effect of the shape of terrain adjacent to the coast must also be considered. Also numerical problems tend to increase because the sea tide has to be discretized on a finer grid to evaluate convolution integrals. Yet coastal areas are most likely to display significant effects.

Because load numbers are defined in almost the same way as Love numbers, the sea-tide effects on individual geodetic quantities are expressed by means of the same linear combinations of corresponding load numbers. Apart from a different potential (W_t replaced by W_w), the main difference is that the equations are applied to all wave numbers, n, and then summed. Alternatively the convolution integrals can be used.

The last topic to be discussed is the selection of independent effects. When we evaluated the pure tidal corrections in the previous sections we did not have to worry that some corrections were dependent on others. The amount of computation needed to evaluate any of these is trivial. However, sea-tide corrections do present a formidable computational effort. Care must be exercised to minimize the duplication of computations. Therefore it appears desirable to select a minimal set of independent effects that can be evaluated (once and for all) for the entire area of interest. The remainder of the effects can then be expressed as simple functions of the minimal set. For example, tilt may be evaluated as a horizontal derivative of vertical displacement and relative vertical displacement as the difference of the two absolute displacements (terrain minus equipotential surface). This may also be a better way to resolve the problem of Green's functions, composed of horizontal derivatives of P_m (cos ψ), discussed earlier.

REFERENCES

Alterman, Z., Jarosch, H., and Pekeris, C. L., 1961: Propagation of Rayleigh waves in the Earth, Geophys. Jour. R.A.S., 4.

Beaumont, C. and Lambert, A., 1972: Coastal structure from surface load tilts, using a finite element model, Geophys. Jour. R.A.S., 29, 203-226.

Bomford, G., 1971: Geodesy. Claredon, Oxford, England, 741 pp.

Condon, E. V. and Odishaw, H., 1958: Handbook of Physics. McGraw-Hill, New York, N.Y., part 3, pp. 3-3 - 3-112.

Doodson, A. T., 1922: The harmonic development of the tide-generating potential, Proc. Roy. Soc. London A., 100, 305-329.

Farrell, W. E., 1972: Deformation of the Earth by surface loads. Rev. Geophysics and Space Phys., 10 (3), 761-797.

Godin, G., 1972: The Analysis of Tides. University of Toronto Press, Toronto, Canada, 264 pp.

Harkrider, D. G., 1970: Surface waves in multi-layered elastic media 2, higher mode spectra and spectral ratios from point source in plane layered earth models, Bull. Seism. Soc. Amer. 60.

Harrison, J. C., 1978: Earth Tides and geodesy. Proceedings of the GEOP-9 Conference, Columbus, Ohio.

Heiskanen, W. A. and Moritz, H., 1967: Physical Geodesy. Freeman, San Francisco, Calif., 372 pp.

Longman, I. M., 1963: A Green's function for determining the deformation of the Earth under surface mass loads, II. Jour. Geophys. Res., 68 (2), 485-496.

Longman, I. M., 1962: A Green's function for determining the deformation of the Earth under surface mass loads, I. Jour. Geophys. Res., 67 (2) 845-850.

Love, A. E. H., 1927: A Treatise on the Mathematical Theory of Elasticity. Cambridge University Press, England, 643 pp.

Melchior, P., 1978: The Tides of the Planet Earth, Pergamon Press, Oxford, England, 620 pp.

Mueller, I. I., 1969: Spherical and Practical Astronomy as Applied to Geodesy. Frederick Ungar Publishing Co., New York, N.Y., 644 pp.

Munk, W. M. and MacDonald, G. F. K., 1960: The Rotation of the Earth. Oxford Press, London, England, 342 pp.

Ozawa, I., 1965: On the Extensometer whose magnifier is a Zöllner suspension type tiltmeter and the observation of the Earth's strains by means of the instruments, Boll. de. Geof. XVIII (3), 263-278.

Rektorys, K. (editor), (1969): Survey of Applicable Mathematics. MIT Press, Cambridge, Mass., 1369 pp.

Vaníček, P., 1973: The tides. Lecture Notes #36, Department of Surveying Engineering University of New Brunswick, Fredericton, N.B., Canada.

Zschau, J., 1976: Tidal sea load tilt of the coast and its application to the study of crustal and upper mantle structures, . Geophys. Jour. R.A.S. 44, 577-593.

(Continued from inside front cover)

NOS NGS-3 Adjustment of geodetic field data using a sequential method. Marvin C. Whiting and Allen J. Pope, March 1976, 11 pp (PB253967). A sequential adjustment is adopted for use by NGS field parties.

NOS NGS-4 Reducing the profile of sparse symmetric matrices. Richard A. Snay, June 1976, 24 pp (PB-258476). An algorithm for improving the profile of a sparse symmetric matrix is introduced and tested against the widely used reverse Cuthill-McKee algorithm.

NOS NGS-5 National Geodetic Survey data: availability, explanation, and application. Joseph F. Dracup, Revised January 1979, 45 pp (PB80 118615). The summary gives data and services available from NGS, accuracy of surveys, and uses of specific data.

NOS NGS-6 Determination of North American Datum 1983 coordinates of map corners. T. Vincenty, October 1976, 8 pp (PB262442). Predictions of changes in coordinates of map corners are detailed.

NOS NGS-7 Recent elevation change in Southern California. S.R. Holdahl, February 1977, 19 pp (PB265-940). Velocities of elevation change were determined from Southern Calif. leveling data for 1906-62 and 1959-76 epochs.

NOS NGS-8 Establishment of calibration base lines. Joseph F. Dracup, Charles J. Fronczek, and Raymond W. Tomlinson, August 1977, 22 pp (PB277130). Specifications are given for establishing calibration base lines.

NOS NGS-9 National Geodetic Survey publications on surveying and geodesy 1976. September 1977, 17 pp (PB275181). Compilation lists publications authored by NGS staff in 1976, source availability for out-of-print Coast and Geodetic Survey publications, and subscription information on the Geodetic Control Data Automatic Mailing List.

NOS NGS-10 Use of calibration base lines. Charles J. Fronczek, December 1977, 38 pp (PB279574). Detailed explanation allows the user to evaluate electromagnetic distance measuring instruments.

NOS NGS-11 Applicability of array algebra. Richard A. Snay, February 1978, 22 pp (PB281196). Conditions required for the transformation from matrix equations into computationally more efficient array equations are considered.

NOS NGS-12 The TRAV-10 horizontal network adjustment program. Charles R. Schwarz, April 1978, 52 pp (PB283087). The design, objectives, and specifications of the horizontal control adjustment program are presented.

NOS NGS-13 Application of three-dimensional geodesy to adjustments of horizontal networks. T. Vincenty and B. R. Bowring, June 1978, 7 pp (PB286672). A method is given for adjusting measurements in three-dimensional space without reducing them to any computational surface.

NOS NGS-14 Solvability analysis of geodetic networks using logical geometry. Richard A. Snay, October 1978, 29 pp (PB291286). No algorithm based solely on logical geometry has been found that can unerringly distinguish between solvable and unsolvable horizontal networks. For leveling networks such an algorithm is well known.

NOS NGS-15 Goldstone validation survey - phase 1. William E. Carter and James E. Pettey, November 1978, 44 pp (PB292310). Results are given for a space system validation study conducted at the Goldstone, Calif., Deep Space Communication Complex.

NOS NGS-16 Determination of North American Datum 1983 coordinates of map corners (second prediction). T. Vincenty, April 1979, 6 pp (PB297245). New predictions of changes in coordinates of of map corners are given.

NOS NGS-17 The HAVAGO three-dimensional adjustment program. T. Vincenty, May 1979, 18 pp (PB297069). The HAVAGO computer program adjusts numerous kinds of geodetic observations for high precision special surveys and ordinary surveys.

NOS NGS-18 Determination of astronomic positions for California-Nevada boundary monuments near Lake Tahoe. James E. Pettey, March, 1979, 22 pp (PB301264). Astronomic observations of the 120th meridian were made at the request of the Calif. State Lands Commission.

NOS NGS-19 HOACOS: A program for adjusting horizontal networks in three dimensions. T. Vincenty, July 1979, 18 pp (PB301351). Horizontal networks are adjusted simply and efficiently in the height-controlled spatial system without reducing observations to the ellipsoid.

NOS NGS-20 Geodetic leveling and the sea level slope along the California coast. Emery I. Balazs and Bruce C. Douglas, September 1979, 23 pp (PB80 120611). Heights of four local mean sea levels for the 1941-59 epoch in California are determined and compared from five geodetic level lines observed (leveled) between 1968-78.

NOS NGS-21 Haystack-Westford Survey. W. E. Carter, C. J. Fronczek, and J. E. Pettey, September 1979, 57 pp. A special purpose survey was conducted for VLBI test comparison.

NOS NGS-22 Gravimetric tidal loading computed from integrated Green's functions. C. C. Goad, October 1979, 15 pp. Tidal loading is computed using integrated Green's functions.

NOS NGS-23 Use of auxiliary ellipsoids in height-controlled spatial adjustments. B. R. Bowring and T. Vincenty, November 1979, 6 pp. Auxiliary ellipsoids are used in adjustments of networks in the height-controlled three-dimensional system for controlling heights and simplifying transformation of coordinates.

NOS NGS-24 Determination of the geopotential from satellite-to-satellite tracking data. B. C. Douglas, C. C. Goad, and F. F. Morrison, January 1980, 32 pp. The capability of determining the geopotential from satellite-to-satellite tracking is analyzed.

Continued on inside cover

(Continued)

NOAA Technical Reports, NOS/NGS subseries

NOS 65 NGS 1 The statistics of residuals and the detection of outliers. Allen J. Pope, May 1976, 133 pp (PB258428). A criterion for rejection of bad geodetic data is derived on the basis of residuals from a simultaneous least-squares adjustment. Subroutine TAURE is included.

NOS 66 NGS 2 Effect of Geoceiver observations upon the classical triangulation network. R. E. Moose and S. W. Henriksen, June 1976, 65 pp (PB260921). The use of Geoceiver observations is investigated as a means of improving triangulation network adjustment results.

NOS 67 NGS 3 Algorithms for computing the geopotential using a simple-layer density model. Foster Morrison, March 1977, 41 pp (PB266967). Several algorithms are developed for computing with high accuracy the gravitational attraction of a simple-density layer at arbitrary altitudes. Computer program is included.

NOS 68 NGS 4 Test results of first-order class III leveling. Charles T. Whalen and Emery Balazs, November 1976, 30 pp (GPO# 003-017-00393-1) (PB265421). Specifications for releveling the National vertical control net were tested and the results published.

NOS 70 NGS 5 Selenocentric geodetic reference system. Frederick J. Doyle, Atef A. Elassal, and James R. Lucas, February 1977, 53 pp (PB266046). Reference system was established by simultaneous adjustment of 1,233 metric-camera photographs of the lunar surface from which 2,662 terrain points were positioned.

NOS 71 NGS 6 Application of digital filtering to satellite geodesy. C. C. Goad, May 1977, 73 pp (PB-270192). Variations in the orbit of GEOS-3 were analyzed for M_2 tidal harmonic coefficient values that perturb the orbits of artificial satellites and the Moon.

NOS 72 NGS 7 Systems for the determination of polar motion. Soren W. Henriksen, May 1977, 55 pp (PB274698). Methods for determining polar motion are described and their advantages and disadvantages compared.

NOS 73 NGS 8 Control leveling. Charles T. Whalen, May 1978, 23 pp (GPO# 003-017-00422-8) (PB286838). The history of the National network of geodetic control, from its origin in 1878, is presented, and the latest observation and computation procedures are explained.

NOS 74 NGS 9 Survey of the McDonald Observatory radial line scheme by relative lateration techniques. William E. Carter and T. Vincenty, June 1978, 33 pp (PB287427). Results of experimental application of the "ratio method" of electromagnetic distance measurements are given for high resolution crustal deformation studies in the vicinity of the McDonald Lunar Laser Ranging and Harvard Radio Astronomy Stations.

NOS 75 NGS 10 An algorithm to compute the eigenvectors of a symmetric matrix. E. Schmid, August 1978, 5 pp (PB287923). Method describes computations for eigenvalues and eigenvectors of a symmetric matrix.

NOS 76 NGS 11 The application of multiquadric equations and point mass anomaly models to crustal movement studies. Rolland L. Hardy, November 1978, 63 pp (PB293544). Multiquadric equations, both harmonic and nonharmonic, are suitable as geometric prediction functions for surface deformation and have potentiality for usage in analysis of subsurface mass redistribution associated with crustal movements.

NOS 79 NGS 12 Optimization of horizontal control networks by nonlinear programing. Dennis G. Milbert, August 1979, 44 pp (PB80 117948). Several horizontal geodetic control networks are optimized at minimum cost while maintaining desired accuracy standards.

NOS 82 NGS 13 Feasibility study of the conjugate gradient method for solving large sparse equation sets. Lothar Grundig, February 1980, 19 pp. This method is well suited for constrained adjustments but not for free adjustments.

NOAA Manuals, NOS/NGS subseries

NOS NGS 1 Geodetic bench marks. Lt. Richard P. Floyd, September 1978, 56 pp (GPO#003-017-00442-2) (PB296427). Reference guide provides specifications for highly stable bench marks, including installation procedures, vertical instability, and site selection considerations.

U.S. DEPARTMENT OF COMMERCE
National Oceanic and Atmospheric Administration
National Ocean Survey
National Geodetic Survey, OA/C18x2
Rockville, Maryland 20852

OFFICIAL BUSINESS

POSTAGE AND FEES PAID
U.S. DEPARTMENT OF COMMERCE
COM-210
THIRD CLASS MAIL